Materials Science & Engineering A 597 (2014) 62–69

Contents lists available at ScienceDirect

Materials Science & Engineering A

journal homepage: www.elsevier.com/locate/msea

Characterization of Al–Li 2099 extrusions and the influence of fiber texture on the anisotropy of static mechanical properties

Alexandre Bois-Brochu [a,*], Carl Blais [a], Franck Armel Tchitembo Goma [a], Daniel Larouche [a], Julien Boselli [b], Mathieu Brochu [c]

[a] Department of Mining and Metallurgy, Adrien-Pouliot Building, Université Laval, 1065 Rue de la medicine, Québec, Québec G1V 0A6, Canada
[b] Alcoa Technical Center, Alcoa, PA 15069, USA
[c] Department of Mining and Materials Engineering, Wong Building, McGill University, 3610 University Street, Montréal, Québec H3A 2B2, Canada

ARTICLE INFO

Article history:
Received 25 July 2013
Received in revised form
16 December 2013
Accepted 16 December 2013
Available online 24 December 2013

Keywords:
Aluminum–lithium
Fiber texture
Anisotropy
Mechanical properties
Microstructure

ABSTRACT

The development of aluminum–lithium alloys for aerospace applications requires a thorough understanding of how processing and product geometry impact their microstructure, texture and mechanical properties. The anisotropy of the mechanical properties is in part related to the deformation texture formed during thermo-mechanical processing. In this study, two different extrusions of Al–Li 2099 T83 were characterized, a cylindrical extrusion and an integrally stiffened panel (ISP). A decrease of tensile properties was observed from the longitudinal direction to the transverse direction with a minimum in the 45° direction, the magnitude of which depends on the location in the extrusions. The ⟨111⟩ fiber texture is prominent in most locations of the extrusion with a smaller intensity of the ⟨100⟩ component. Rolling textures were observed in two locations of the ISP that have a larger cross sectional aspect ratio. Variations of strength and anisotropy as a function of location in the extrusion correlate well with the intensity of the ⟨111⟩ fiber texture. On the other hand, our findings show an absence of correlation between the Taylor factor and the anisotropy. These results suggest that strength anisotropy may be controlled by the volume fraction of T_1 precipitates that could itself be related to the intensity of the ⟨111⟩ fiber texture.

© 2013 Elsevier B.V. All rights reserved.

1. Introduction

Aluminum–lithium alloys are increasingly replacing traditional aluminum alloys in aerospace applications. The interest in using these alloys comes primarily from the lower density and higher stiffness they provide. The density of the alloy is lowered by 3% for every weight percent of lithium added and stiffness is increased by 5–6% per weight percent of Li. The lower density combined with equal or improved strength gives these alloys improved specific properties over traditional aluminum alloys [1,2]. Such improvements can lead to reductions in fuel consumption and provide an opportunity to compete with composites in airplane designs [3].

In the past, lithium containing alloys were characterized by high levels of anisotropy of mechanical properties caused by deformation textures created during shaping [4]. Second generation Rolled Al–Li products were characterized with having high intensities of the Brass texture component high in-plane anisotropy [3–5]. In the case of aluminum products shaped with smaller aspect ratios such as those found in cylindrical extrusion or drawn tube, ⟨111⟩ and ⟨100⟩ fiber textures are developed with the predominance of the ⟨111⟩ texture due to the high stacking-fault energy of aluminum [5,6]. The presence of fiber texture causes axisymmetric flow anisotropy (AFA) [5–8]. Both the AFA and in-plane anisotropy cause a decrease in strength at orientations other than the main deformation direction, particularly for intermediate angles nearing 45° from the longitudinal direction [1,3,4,9–11]. Axisymmetric flow anisotropy also leads to a reduction of the differences between yield strength and ultimate tensile strength. For aerospace applications, low strength in off axis directions may negate the benefits of high strength in the working direction for some applications [4]. For applications where the principal stress aligns with the working direction (wing skins, wing and fuselage stringers), 45° properties are less of a concern. Thus, new aluminum–lithium alloys must be characterized thoroughly in terms of texture, static mechanical properties and anisotropy. Therefore, the main objective of the work summarized in this paper is to carry out such characterization for two types of extrusions produced with Alcoa's 2099 alloy in the T83 temper. The chemical composition of this alloy can be found in Table 1,

* Corresponding author. Tel.: +1 819 376 8707x42.
E-mail addresses: Alexandre.Bois-Brochu.1@ulaval.ca (A. Bois-Brochu), Carl.Blais@gmn.ulaval.ca (C. Blais), Franck-Armel.Tchitembo-Goma.1@ulaval.ca (F.A.T. Goma), Daniel.Larouche@gmn.ulaval.ca (D. Larouche), Julien.Boselli@alcoa.com (J. Boselli), Mathieu.Brochu@mcgill.ca (M. Brochu).

0921-5093/$ - see front matter © 2013 Elsevier B.V. All rights reserved.
http://dx.doi.org/10.1016/j.msea.2013.12.060

Table 1
Chemical composition for the 2099 alloy (wt%) [3].

Cu	Li	Zn	Mg	Mn	Zr	Ti	Fe	Si	Be	Al
2.4–3.0	1.6–2.0	0.4–1.0	0.1–0.5	0.1–0.5	0.05–0.12	0.1 Max	0.07 Max	0.05 Max	0.0001 Max	Balance

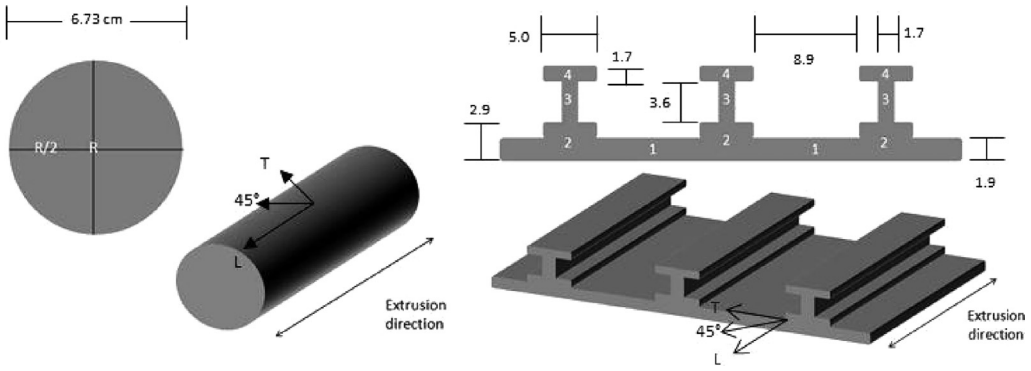

Fig. 1. Cylindrical extrusion (left) and integrally stiffened panel (ISP) (cm) (right).

while Fig. 1 presents the two extrusions that were studied. The extrusion in Fig. 1 (left) is cylindrical with an extrusion ratio of 21.4 whereas the one in Fig. 1 (right) is an integrally stiffened panel (ISP) with an extrusion ratio of 15.7. The important locations in the ISP are the web (1), the stiffener base (2), the stiffener web (3) and the stiffener cap (4).

2. Methodology

Specimens were taken at the center of the cylindrical extrusion (R) and at half the radius ($R/2$) while four locations were selected for specimen sampling in the ISP: middle of the web and the stiffener base (1 and 2), the stiffener web (3) and the stiffener cap (4). Microstructural characterization was carried out using optical microscopy and electron backscattered diffraction (EBSD). The latter was used for grains and sub-grains characterization using lattice misorientation angles to differentiate one from the other. The SEM used with EBSD was a Hitachi S-4700 with EBSD HKL Nordyls and Flamenco acquisition system. Areas of 0.05 mm^2 were analyzed with EBSD. Composition and distribution of second phase particles were analyzed. Chemical compositions of the particles were obtained using energy-dispersive X-ray spectrometer (EDS) of the PGT brand installed on a JEOL 840-A SEM. Second phase particles were also analyzed using a CAMECA SX-100 microprobe analyzer for quantitative measurement. Characterization of the distribution of particles was done using mirror finish polished samples. For the cylindrical extrusion, 200 micrographs of 26,512 μm^2 each were used, going from the sample surface toward its center, always in the longitudinal direction. For the ISP, 74 micrographs per location were used, going from one side of the extrusion to the other with the longitudinal direction in the plane. For the fine characterization of precipitates, a TEM JEOL JEM-2100F was used.

For quantitative macrotexture analysis, X-ray diffraction was selected using a Bruker Discover D8 with a HISTAR zone detector and the data analysis program used was Tex tools. The area of the surface analyzed in XRD was 4 mm^2. Fiber textures intensities were quantified in terms of their peaks on inverse pole figures.

Static mechanical properties were determined using a SATEC T20000 universal testing machine. The properties were characterized along the longitudinal direction (L), the transverse direction (T) and at 45° from these directions (45). Two series of cylindrical tensile specimens were used. The first one had a gauge diameter of 0.287 cm while the second type had a diameter of 0.406 cm. For both specimen types, the gauge length was 1.27 cm. The crosshead speed used was in accordance with ASTM E8 standard and was 2 mm/min. Compression test specimens with a height of 1.09 cm and a diameter of 0.635 cm were also prepared. The crosshead speed used was 2 mm/min. The tensile and compression tests were both conducted at room temperature. Five specimens per orientation were tested for each location.

3. Microstructure

The extruded alloy contains a mostly unrecrystallized microstructure. This is due in part to dynamic recovery during the hot extrusion but also due to the presence of Al_3Zr (β') coherent particles that minimize recrystallization through Zener drag during solution heat-treatment, thus maintaining substructure strengthening [1,4,5,8,12]. Following hot working, aluminum alloys usually present a microstructure with elongated grains with subgrains. This behavior at hot working temperature is due to the high stacking-fault energy known for aluminum [5]. However, static recrystallization can still occur after hot working under certain circumstances such as solution heat treatment in areas where severe strains have occurred such as immediately below the surface of the extrusion [5,8]. This would apply here in the case of heat-treated 2099 T83 extrusions where high strains are expected near the surface [8]. Fig. 2 presents the elongated grain structure observed in the ISP Section 2. A similar elongated microstructure was observed in the other sections of the ISP and the cylindrical extrusion. In Fig. 3, it is possible to see the evolution of the grain structure from the center to the surface of the cylindrical extrusion, in the transverse direction. The grains are roughly equiaxed in the center as opposed to those located at half the radius, as seen in Fig. 3(b), where the elongation of the grains is caused by the increased shear during the flow from center to the surface of the extruded product. In Fig. 3(c), small recrystallized grains can be observed near the surface of the cylindrical extrusion. This is due to the severe deformation near the surface. Even if dynamic recovery occurred and Al_3Zr are present, the driving force for recrystallization [5] is high enough near the surface, so static recrystallization occurs. Large grains are often observed in this situation, but in this case, the Al_3Zr dispersoids appear to have

Download English Version:

https://daneshyari.com/en/article/7981327

Download Persian Version:

https://daneshyari.com/article/7981327

Daneshyari.com